infrastructures

MDPI

Article

A Creep Prediction Model for Concrete Made from Pit Sand with Low Silica Content

Daud Andang Pasalli [1,2,*], Sri Tudjono [2] and Ilham Nurhuda [2,*]

[1] Departement Civil Engineering, Musamus University, Merauke 99600, Indonesia
[2] Departement Civil Engineering, Diponegoro University, Semarang 50275, Indonesia
* Correspondence: daudap@unmus.ac.id (D.A.P.); ilham@live.undip.ac.id (I.N.)

Abstract: Pit sand generally has a lower silica content than sand sourced from rivers or crushed stones. The effect of this sand on the creep of concrete has not yet been fully studied. Understanding the creep of concrete can help to estimate the behaviour of structures in the future. This study aimed to investigate the effects of the properties of pit sand with different chemical compositions and grain size distributions on the creep of concrete, and to develop a creep prediction model for concrete made of pit sand with low silica content. This investigation employed laboratory testing to obtain the physical and chemical properties of the sand, and its relationship to the shrinkage and creep of concrete. A concrete creep prediction model is proposed based on the modification of the B3 Model. Modifications were made by proposing a material constant obtained from short creep tests. The creep parameter obtained from the test can be better used to predict the creep of concrete.

Keywords: pit sand; concrete; creep; model

Citation: Pasalli, D.A.; Tudjono, S.; Nurhuda, I. A Creep Prediction Model for Concrete Made from Pit Sand with Low Silica Content. *Infrastructures* **2022**, *7*, 134. https://doi.org/10.3390/infrastructures7100134

Academic Editors: Kevin Paine

Received: 28 August 2022
Accepted: 30 September 2022
Published: 5 October 2022

1. Introduction

The development of infrastructures often requires local construction materials to reduce construction costs. One of the local materials frequently used in construction is pit sand from nearby sources. However, pit sand is still rarely used as a building material, although it is widely distributed around the world. Pit sand generally comes from sedimentary materials and weathered rocks which form the Earth's surface layer. The characteristics and properties of pit sand are highly dependent on the chemical compositions of its constituents. In some cases, this type of sand has a lower silica content than sand sourced from rivers or crushed stones.

The quality of concrete is often specified by its compressive strength (fc'). This strength represents its capability to resist a short duration of compressive loading. However, in many cases, structures must withstand long-duration loading or even sustained loading. In this condition, the creep and shrinkage properties of the concrete will determine the performance of the structure [1,2].

The use of local sand as concrete has been investigated by some researchers [3–7]. However, little can be found on the modelling of creep deformation of concrete made from local sand [7]. This study aimed at investigating the effects of the properties of pit sand with different chemical compositions and grain distributions on the creep of concrete. A concrete creep prediction model is proposed based on the results of this study.

2. Materials and Methods

2.1. Sand

This research investigated pit sand taken from Merauke Regency in Indonesia, which is geographically located in the far south of Papua Province, near the border with Papua New Guinea. Concrete in Merauke Regency is normally made from sand brought from

other islands, which increases the cost of infrastructure in Merauke. In this study, pit sand was taken from three local sources in Merauke Regency, namely, Tanah Miring, Malind and Kurik Districts.

The properties of pit sand from Merauke were examined to study the effects of its properties on the resulting concrete. The physical properties of pit sand studied in this research were grain size distribution, fineness modulus, bulk density, specific gravity, water absorption, and also mud and organic content. The chemical composition of pit sand was examined using the X-ray fluorescence (XRF) method.

The material properties of Merauke pit sand are shown in Table 1. It can be seen that sands from Malind and Tanah Miring districts have higher fineness moduli compared to sand from the Kurik district, meaning that Malind and Tanah Miring sands tend to have a larger grain size. Sand with coarse gradations tends to have higher porosity due to the lack of finer materials to fill the gaps between the larger grains. However, the sand from the three locations still meets the requirements for grain gradation of sand.

Table 1 shows the specific gravity values of the pit sand varied from 2.52 to 2.96; the highest specific gravity was owned by Kurik sand. The water absorption of sand ranged from 2.43% to 3.19%; the highest rate was for the Tanah Miring sand. The percentage of fine grains, that is, sand with a grain size less than 75 μm (passed through the No. 200 sieve), ranged from 0.35% to 3.44%, whereas the mud content ranged from 3.13% to 4.9%. Sand from the Tanah Miring area showed a higher percentage of fine grains and a higher percentage of mud content than sand taken from other locations. However, the percentage of mud content was still below the requirements specified in the code [8].

Table 1. Physical properties of pit sand.

Properties	Unit	Kurik Sand (KS)	Malind Sand (MS)	Tanah Miring Sand (TS)
Fineness modulus of grain size		3.594	3.645	3.644
Specific gravity		2.96	2.52	2.69
Water absorption	%	2.60	2.43	3.19
Percentage of fine grains	%	0.64	0.35	3.44
Percentage of mud	%	3.13	4.58	4.90

The major chemical compounds found in the pit sand are shown in Table 2. The results show that silica oxide (SiO2), iron oxide (Fe2O3), calcium oxide (CaO) and alumina oxide (Al2O3) are the four major chemical compounds found in the sand. Table 2 shows that pit sand from the three sources had smaller percentages of silica to sand normally used in building construction [9]. The largest percentage of silica oxide was only 52.2%, which was found in Tanah Miring sand. This investigation also found that pit sand from the three sources contains a large percentage of iron oxide; together, silica oxide and iron oxide make up 75.5–93.4% of the chemical compounds in Merauke pit sand. Additionally, sand from the Malind district had the highest CaO content compared to those from other locations. CaO is one of the main components of cement. Hence, its content needs attention, as it can affect the properties of the resulting concrete.

Table 2. Chemical compounds in pit sand.

Chemical Compound	Unit	Kurik Sand (KS)	Malind Sand (MS)	Tanah Miring Sand (TS)
Silica Oxide—SiO_2	%	28.70	37.30	52.20
Iron (III) Oxide—Fe_2O_3	%	64.70	38.20	34.80
Calcium Oxide—CaO	%	0.26	13.40	0.14
Alumina Oxide—Al_2O_3	%	4.75	1.97	8.90
Other compounds	%	1.59	9.13	3.96

2.2. Mortar

Mortar specimens had a constant weight ratio of cement to sand of 0.5, and the cement water factor was 0.4 for each mixture. There was a total of 27 mortar specimens for compressive strength and water absorption tests. All mortar specimens were cubes of size 50 mm × 50 mm × 50 mm. The test results in Table 3 show the variation in the compressive strength of the mortar, ranging from 24.70 to 40.68 MPa, and the water absorption of the three types of sand was small, below 2.5% in the first 10 min, and below 6% in 24 h.

Results from the material test show that the sand sourced from the three locations meets the requirements for use in structural concrete. Hence, pit sand from the three locations could be used to make concrete specimens for further tests.

Table 3. Compressive strength and water absorption of cement mortar.

Properties	Unit	Kurik Sand (KS)	Malind Sand (MS)	Tanah Miring Sand (TS)
Compressive strength of cement mortar	MPa	40.68	38.41	24.70
10 min water absorption	%	0.37	0.35	0.42
24 h water absorption	%	1.90	1.73	2.06

2.3. Coarse Aggregates

The coarse aggregates used in this study were of crushed stones sourced from outside Merauke. The size of crushed stones varied from 10 to 20 mm and had bulk specific gravity of 2.66. The crushed stones had an average SSD water content of 1.2% and a mud content of 0.55%. These crushed stones were used in all specimens. Hence, the variations in results in this investigation were expected to only come from the different types of sand.

2.4. Concrete

The concrete specimens were designed to have a compressive strength of 30 MPa and a water–cement factor of 0.4. The amount of cement was taken as a constant of 500 kg/m^3 for all specimens to simulate the maximum creep of concrete. The amount of water was 200 kg/m^3, which was calculated based on the designed water–cement factor of 0.4.

Concrete specimens were made from pit sand from the three locations, namely, Kurik, Malind and Tanah Miring districts in Merauke Regency of Indonesia. The compositions of the concrete mixtures are shown in Table 4.

Table 4. Mix proportions of concrete and number of specimens.

Materials and Number of Specimens	Unit	Kurik Concrete (BK)	Malind Concrete (BM)	Tanah Miring Concrete (BT)
Portland cement	Kg/m^3	500.0	500.0	500.0
Sand	Kg/m^3	679.3	671.5	676.7
Coarse aggregate	Kg/m^3	1016.9	1016.9	1016.9
Water	Kg/m^3	200.0	200.0	200.0
w/c	-	0.4	0.4	0.4
Number of Specimens for Compressive Strength and Modulus of Elasticity Test	Specimens	3	3	3
Number of Specimens for Creep Test	Specimens	3	3	3
Number of Specimens for Shrinkage Test	Specimens	3	3	3

The concrete specimens were prepared for four types of tests, namely, the modulus of elasticity, compressive strength, shrinkage and creep of concrete tests. Each type of test was carried out on the concretes made of sand from the three locations. All test specimens were cylindrical with a diameter of 150 mm and a height of 300 mm. All specimens underwent the same treatment, such as moist curing, and were stored in room conditions at the same temperature and relative humidity [10,11].

2.5. Methods

The compressive strength and modulus of elasticity tests were conducted using a universal testing machine (UTM) equipped with a load cell to read the load. Concrete strain was measured using a strain gauge mounted on the surface of the concrete cylinder. The focus of this test was to obtain the maximum load and the stress–strain relationship up to the maximum load for determining the modulus of elasticity of the concrete. The test setup is as shown in Figure 1.

Shrinkage tests were carried out to calculate the effect of shrinkage on the calculation of creep deformation. The shrinkage tests were carried out by installing dial gauges on the top side of each cylinder, as shown in Figure 2. The shrinkage tests were conducted on three specimens for each type of concrete.

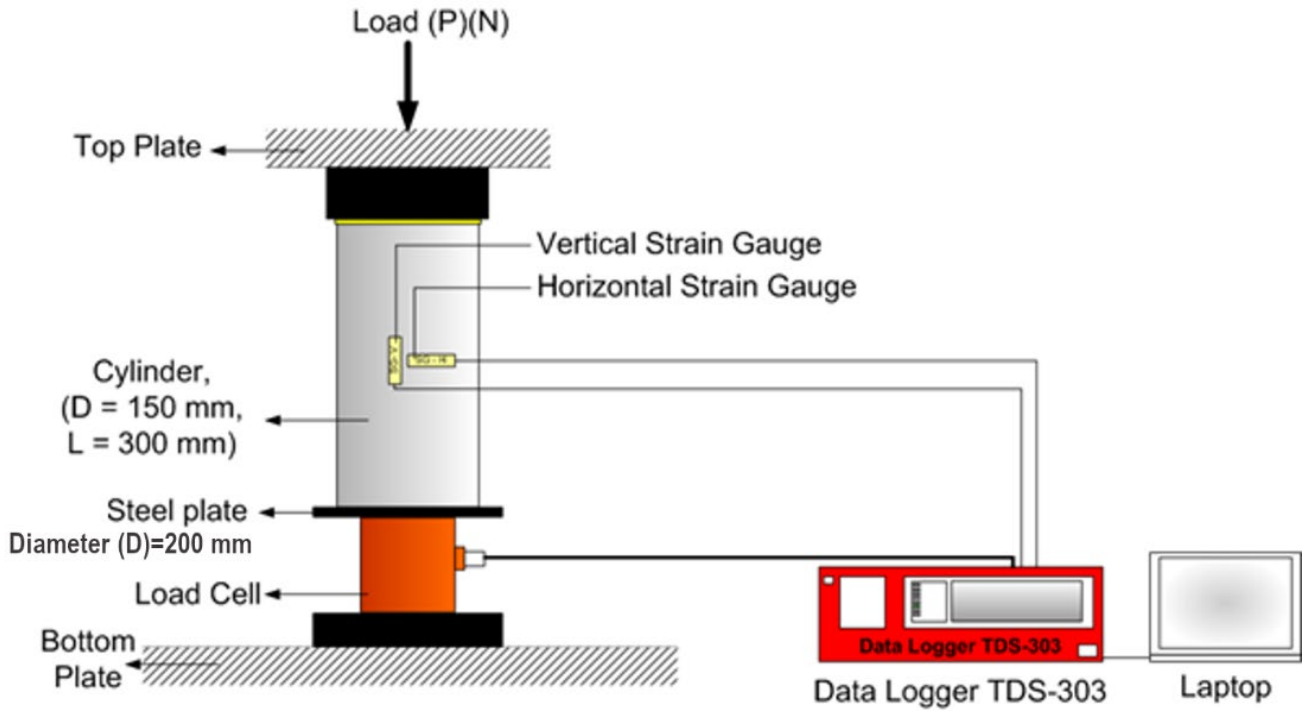

Figure 1. Test setup for compressive strength and elasticity modulus.

Figure 2. The measurement of shrinkage deformation.

The creep test was carried out by applying a constant load of 25% of the maximum load that can be carried by the concrete cylinder based on the compressive strength of concrete. The loading mechanism involved fixed loading with a steel ballast to ensure the load did not change during the test, as shown in Figures 3 and 4. Deformation measurements were carried out simultaneously on three concrete specimens made from the same sand. The specimens were arranged in series to ensure that they received the same load, as shown in Figure 4. The creep deformation was the average value of the measurements from the three specimens [11].

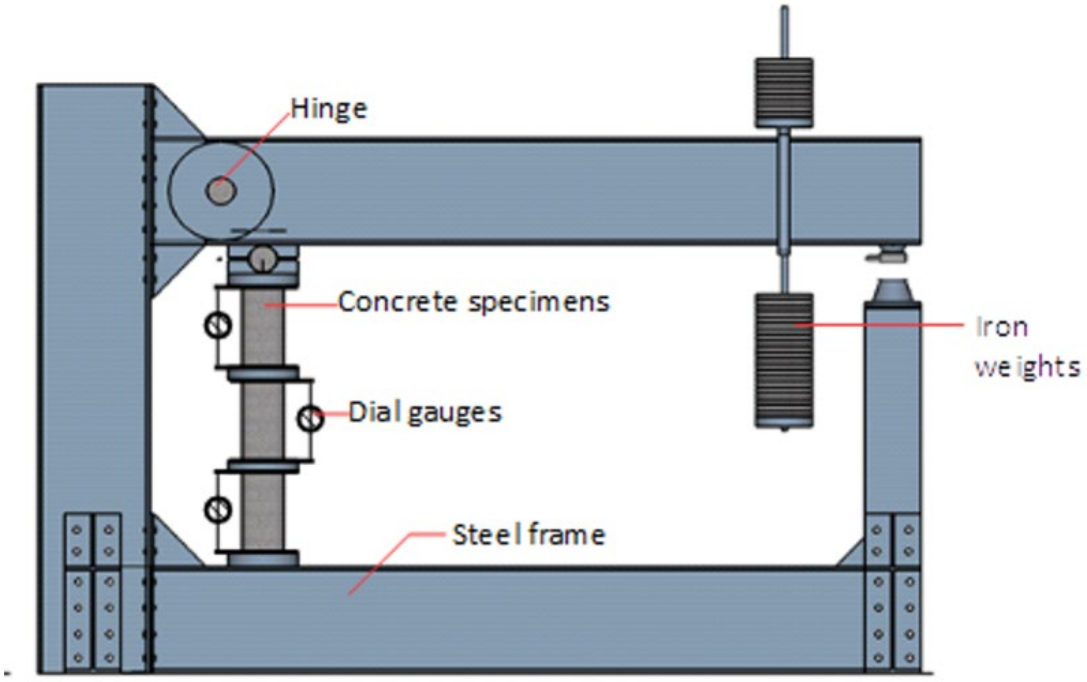

Figure 3. Setup for creep test.

Figure 4. Displacement measurements of concrete creep.

3. Results and Analysis

3.1. Compressive Strength of Concrete

The compressive strength and the elasticity modulus of concrete were obtained by pressing the specimens until the maximum load was reached. The stress–strain relationship of each concrete up to the maximum load is shown in Figure 5. The elasticity modulus of concrete was taken as the slope of the line up to 40% of the maximum stress. Specimens BK and BM had similar stiffness, as shown in Figure 5, and elasticity moduli (Table 5), whereas specimen BT exhibited a much lower elasticity modulus.

Table 5. Compressive strength and elasticity modulus of each concrete.

Concrete Specimens	Compressive Strength (MPa)	Modulus of Elasticity (MPa)
BK	34.5	25,357
BM	31.3	22,210
BT	15.3	13,377

The compressive strength of each type of concrete and the value of its modulus of elasticity are presented in Table 5. The compressive strength of the concrete was comparable to the compressive strength of the mortar in the material test shown in Table 3. Mortar with higher compressive strength will provide concrete with high compressive strength, and vice versa. The compressive strength of specimen BT, which was made from Tanah Miring sand, was the lowest amongst the specimens. The low elasticity modulus and compressive strength of Tanah Miring concrete were because of the high percentages of fine grains and mud found in the sand [12,13].

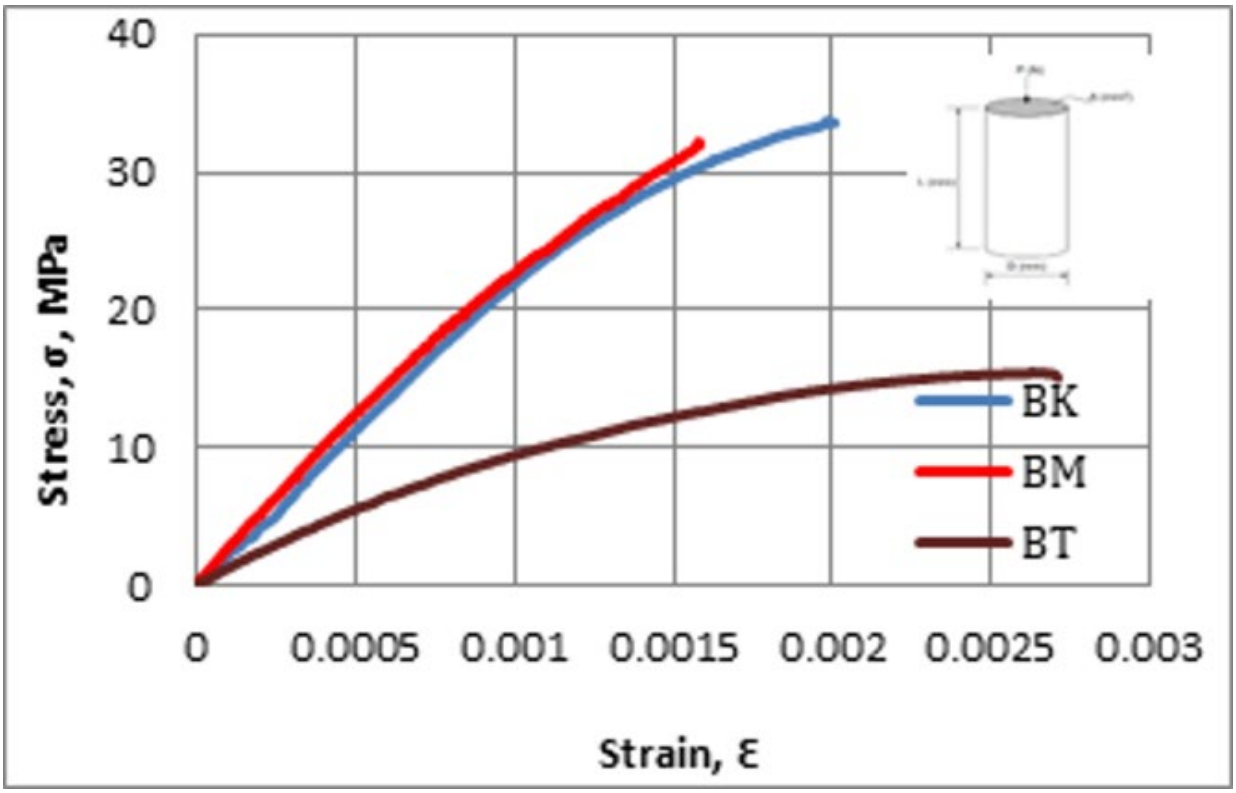

Figure 5. Stress–strain relationship of concrete.

3.2. Shrinkage of Concrete

The measurements of shrinkage deformation were carried out simultaneously with the creep deformation ones. The shrinkage strains were calculated by dividing shrinkage deformation by the initial length, and the measurements were carried out for 364 days. The shrinkage strain graph over time is presented in Figure 6, which shows that Tanah Miring concrete had the largest shrinkage strain. The water absorption test data (Table 1) show that Tanah Miring sand had the largest water absorption, followed by Kurik sand and Malind sand. It can be seen that the water absorption of sand is correlated with the shrinkage deformation. Concrete made from sand with high water absorption has a high shrinkage value. On the other hand, concrete made of sand with low water absorption has a small shrinkage value [13–15].

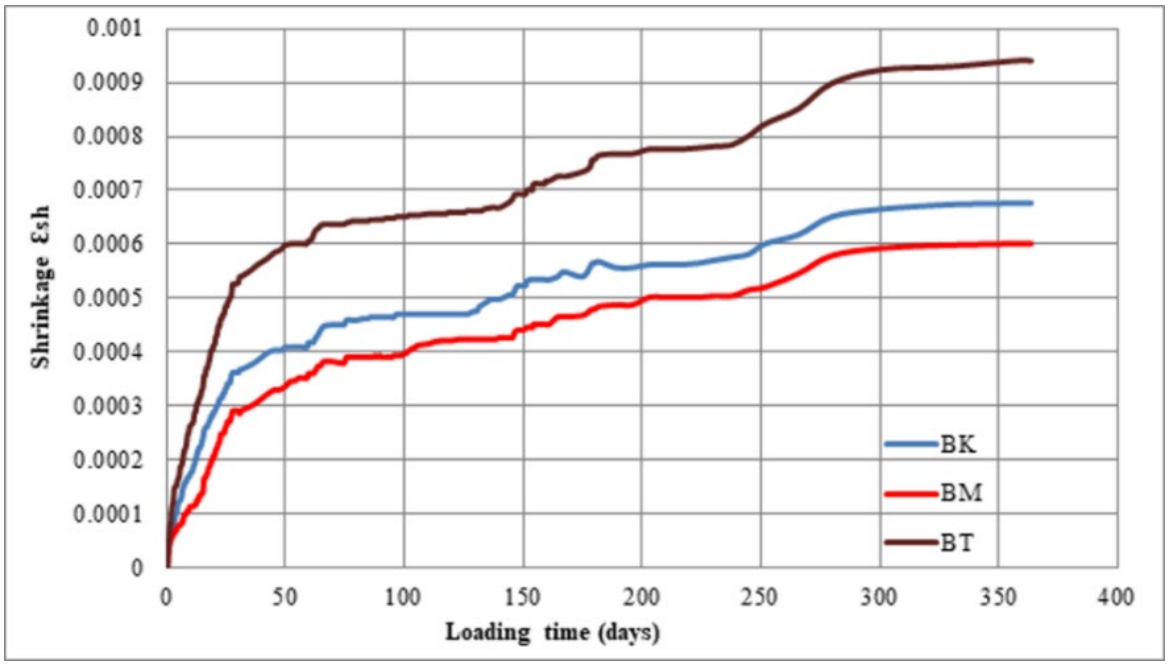

Figure 6. Development of shrinkage strains over 364 days.

Results from X-ray fluorescence (XRF) tests show that sand from the Malind district contains more CaO than other sand, as shown in Table 2. It is known that the amount of water used in the hydration process is not as much as the amount of water given in the mix design. The unused water will evaporate and cause drying shrinkage [16–18]. As CaO reacts with water, sand that contains more CaO requires more water, and the amount of remaining water becomes less. Hence, the shrinkage of concrete made from sand with high CaO content is less than that of other specimens.

Figure 6 shows that the curve of shrinkage strain after 300 days tends to be flat, which indicates a relatively small increase in shrinkage strain after that time. Figure 6 also shows that the shrinkage strain of concrete early on is the highest. The shrinkage strain value up to about 28 days greatly affects the overall shrinkage strain because it contributes to about half of the final shrinkage strain value. The 28-day figure is important because it can be used to carry out tests in a relatively shorter time, and the results can used to make estimates of the final shrinkage strain.

3.3. Creep on Concrete

Creep cannot be measured directly but can be determined by subtracting from the total strain the elastic strain and shrinkage strain, as shown in Equation (1) [10,11]. The readings of strain on the creep test were recorded two to six hours after the loading start, every day for a week, every week for a month, and every month for up to a year [11].

$$\varepsilon_{cc} = \varepsilon_t - \varepsilon_e - \varepsilon_s \quad (1)$$

where ε_{cc} is creep strain, ε_t is total strain, ε_e is elastic strain and ε_s is shrinkage strain. The total strain ε_t is calculated using the following equation:

$$\varepsilon_t = \frac{\Delta L_{rt}}{Lo_{rt}} \quad (2)$$

where ΔL_{rt} is length change measured by dial gauges and Lo_{rt} is initial length.

The measurement data of total strain (ε_t) for 364 days are shown in Figure 7. It shows that Tanah Miring concrete (BT) had the highest total strain, followed by Kurik concrete (BK) and Malind concrete (BM). The creep strain (ε_{cc}) could be calculated using Equation

(2) after the total strain (ε_t) and shrinkage strain (ε_s) were obtained from the measurements.

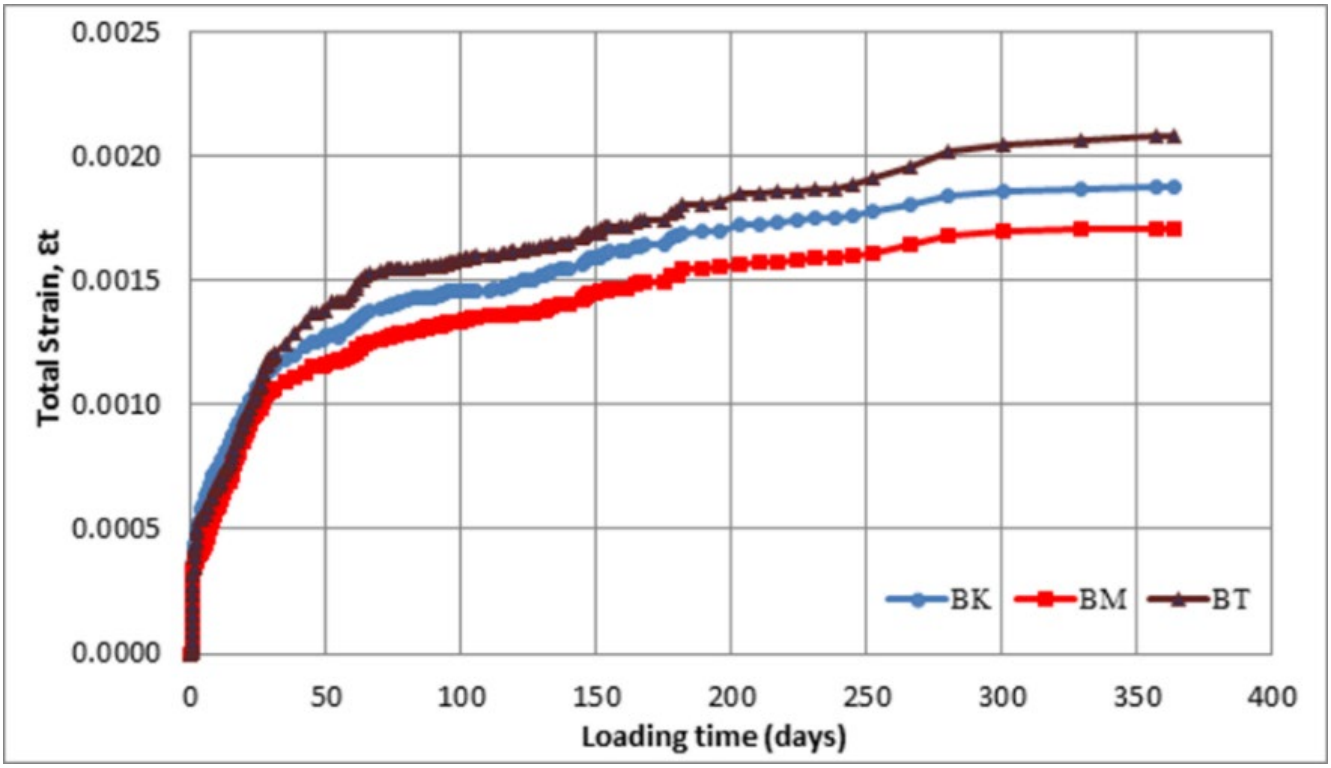

Figure 7. Total strain after sustained loading for 364 days.

Creep is a long-term strain under constant stress which is dependent on time and will result in additional elastic strain for the concrete [10]. Creep can be estimated using a creep coefficient $\phi_{cc}(t)$, as shown in Equation (3). The creep coefficients obtained from this research are shown in Figure 8.

$$\varepsilon_{cc.t} = \emptyset_{cc.}(t)\ (\ \varepsilon_e\ ) \quad (3)$$

Creep measurement for 364 days after loading showed that the creep of Tanah Miring concrete (BT) was higher than those of Malind concrete (BM) and Kurik concrete (BK). This result confirms the effect of elasticity modulus on the creep of concrete, in which concrete with a low elastic modulus has a higher creep strain [2]. This phenomenon was also seen in Malind concrete and Kurik concrete: Malind concrete that has a smaller modulus of elasticity to Kurik concrete exhibits a higher creep coefficient than Kurik concrete.

Results from the physical testing (Table 1) show that Tanah Miring sand has a percentage of fine grains of 3.4%, which is far higher than the percentages of other sands, which ranged from 0.3% to 0.6%. It is known that a large number of fine grains can increase concrete creep [19,20]. In addition, Table 1 shows that Kurik concrete has the lowest mud content, which contributes positively to preventing high creep [20–22].

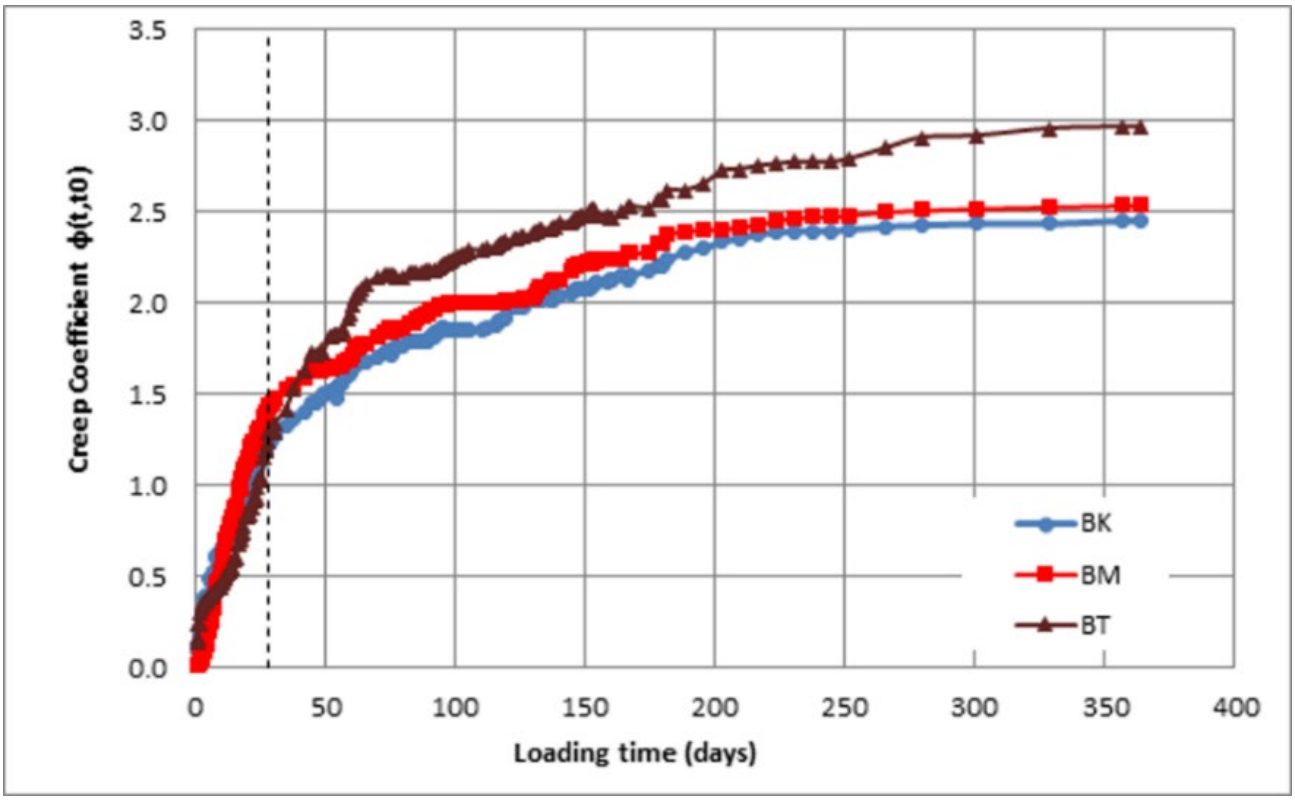

Figure 8. Creep coefficient.

Figures 6 and 8 show similar trends in the shrinkage graph and the creep graph. The similarity between the two graphs confirms the strong relationship between concrete shrinkage and creep [23,24]. It is also seen in Figure 8 that the creep coefficient increases rapidly at an early age. However, the creep coefficient is relatively constant without any large increase in strain after the loading duration reaches 300 days. The rapid creep strain at an early age gives the potential for creep testing in a short timeframe, and then creep predictions can be calculated based on the results of the measurement. The definition of early age is relative, but it can be taken to be approximately 28 days, as shown by a dashed line in Figure 8, which indicates a reasonable estimate.

4. Discussion

4.1. Creep Prediction Model for Concrete

Creep prediction in concrete has been studied for decades [7,25–31]. Creep prediction models have even been included in codes of practice [10,31]. However, the existing models cannot be applied to materials in all areas. Concrete made from Merauke sand, which has low silica content and high iron oxide content, cannot be well predicted by available creep models. The existing creep prediction models showed large discrepancies when they were applied to the concrete specimens in this study. Hence, a modification to existing models was needed for predicting the creep of concrete made from Merauke sand.

One of the complete creep models is the B3 Model [27,28]. This model takes into consideration many aspects to estimate creep in concrete, including the water–cement ratio, the cement content, the ratio of aggregate to cement, the compressive strength and elasticity modulus of the concrete, the concrete age and duration of loading, the concrete stress during loading, the shape and surface area of the concrete and relative humidity. Other aspects are calculated using the main data. Although the B3 Model has not been able to accurately model the creep in Merauke concrete, this model is flexible enough to be modified based on the behaviour of the existing concrete specimens. Hence, modification of the B3 Model was carried out for estimating creep in Merauke concrete.

4.2. Modification of the B3 Model

The Bazant-Baweja B3 Model uses a compliance function $J(t, t_0)$ to reduce the risk of error due to an inaccurate modulus of elasticity. This model separates the basic creep and drying shrinkage [25,28]. In this study, the B3 Creep Model was modified to account for the different properties of sand. One important parameter in the B3 Model is the shrinkage half-time (τ_{sh}) in Equation (4). The shrinkage half-time (τ_{sh}) formula in Equation (4) was modified to Equation (5), in which K_{hs} is a half-shrinkage constant calculated based on the results of creep measurements at a short duration.

$$\tau_{sh} = 0{,}085\, {t_c}^{-0{,}08}\, {f_{cm28}}^{-0{,}25}\, [2k_s(V/S)]^2 \quad (4)$$

$$\tau_{sh} = K_{hs}\, {t_c}^{-0{,}08}\, {f_{cm28}}^{-0{,}25}\, [2k_s(V/S)]^2 \quad (5)$$

where t_c is loading time (days), f_{cm28} is the 28-day standard cylinder compressive strength of concrete, k_s is the cross-section shape factor and V/S is the volume-to-surface ratio of the specimens.

The results of this study show that the creep coefficient increases rapidly at an early age of up to 28 days, as shown in Figure 8. Hence, the creep parameter of shrinkage half-time (τ_{sh}) was studied at 28 days of loading. To take into account the variation in measurement results, the calculation was carried out for 27, 28, and 29 days of age, and then the average was taken.

The procedure for modifying the B3 Model based on the results of the creep test is as follows:

a. Calculate compliance function $J(t, t_0)$ based on the creep coefficient value $\emptyset(t, t_0)$ from the measurement results and the elasticity modulus of concrete at the beginning of test, $E(t_0)$, using the relationship in Equation (6).

$$J(t, t_0) = \frac{\emptyset(t, t_0) + 1}{E(t_0)} \quad (6)$$

b. Calculate the instantaneous compliance q_1 and the compliance function for basic creep $C_0(t, t_0)$ [28].

c. Calculate compliance function for drying creep $C_d(t, t_0, t_c)$ based on the values of $J(t, t_0)$, q_1 and $C_0(t, t_0)$ using Equation (7).

$$C_d(t, t_0, t_c) = J(t, t_0) - q_1 - C_0(t, t_0) \quad (3)$$

d. Calculate the value of shrinkage half-time (τ_{sh}) that meets the value of $C_d(t, t_0, t_c)$ [28].

Figure 9 shows the value of compliance functions $J(t, t_0)$, for 27 to 29 days of age, for concrete made from three types of local sand in Merauke. Tanah Miring concrete (BT) shows higher compliance function $J(t, t_0)$ values compared to other specimens. The value of compliance function $J(t, t_0)$ were then used to calculate the value of the compliance function for drying creep $C_d(t, t_0, t_c)$, as shown in Figure 10. It shows that the compliance function for drying creep $C_d(t, t_0, t_c)$ of Malind concrete (BM) is higher than those of other specimens.

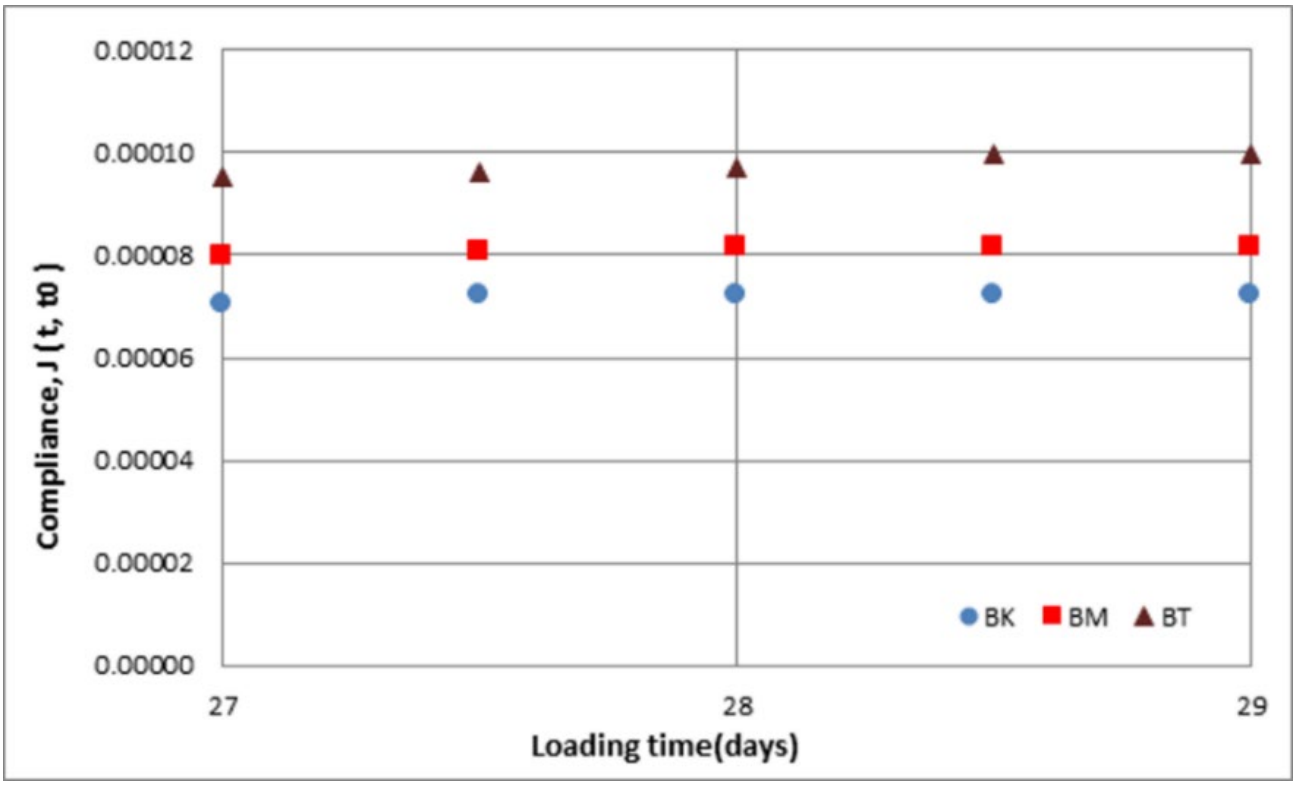

Figure 9. Compliance function $J\left(t, t_0\right)$ at 27–29 days of loading.

The calculated values of shrinkage half-time (τ_{sh}) are presented in Figure 11, which shows the variation in shrinkage half-time (τ_{sh}) for each specimen. The shrinkage half-time (τ_{sh}) in Table 6 was calculated from the average value of shrinkage half-time (τ_{sh}) for each concrete. In this modified version, the estimation of shrinkage half-time (τ_{sh}) in Equation (4) is expanded to Equation (5) by including the constant K_{hs} as a material property. The value of K_{hs} can be calculated using the average shrinkage half-time (τ_{sh}) value in Table 6, and the results are written in Table 6.

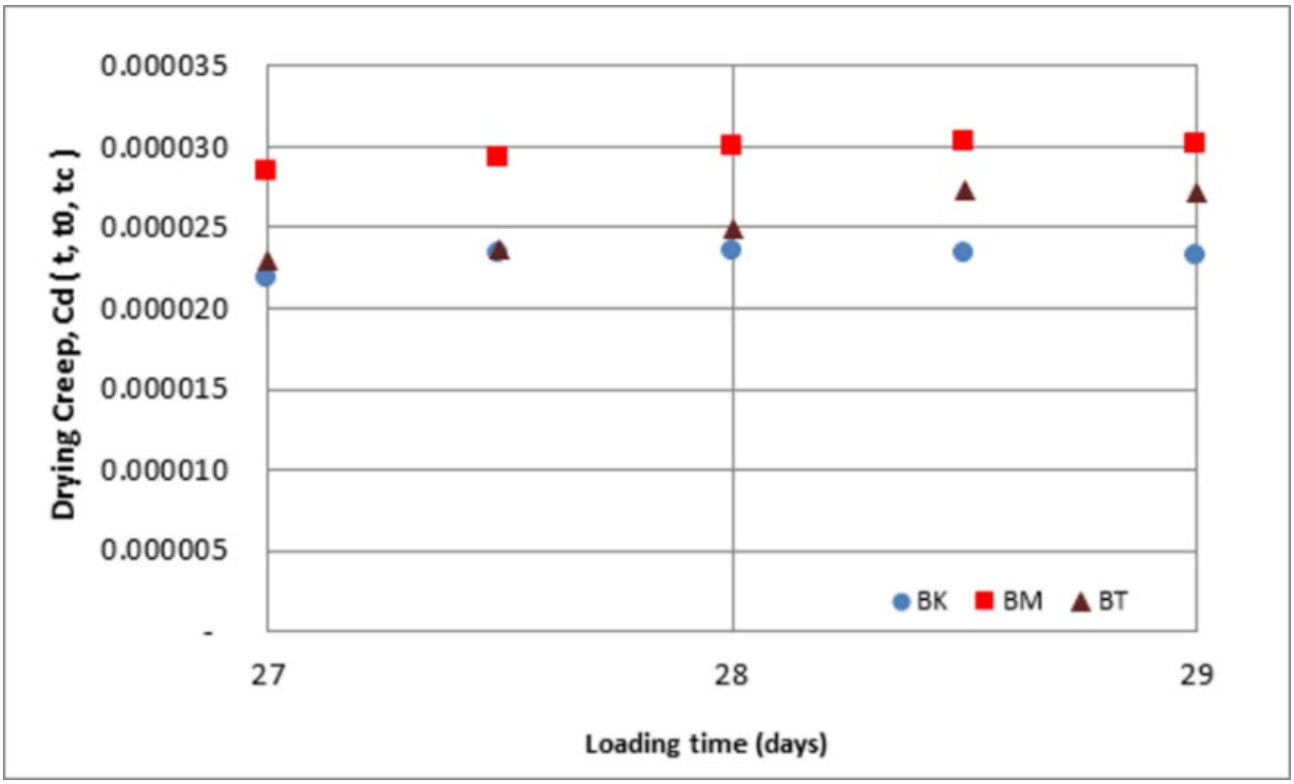

Figure 10. Compliance functions for drying creep $C_d(t, t_0, t_c)$.

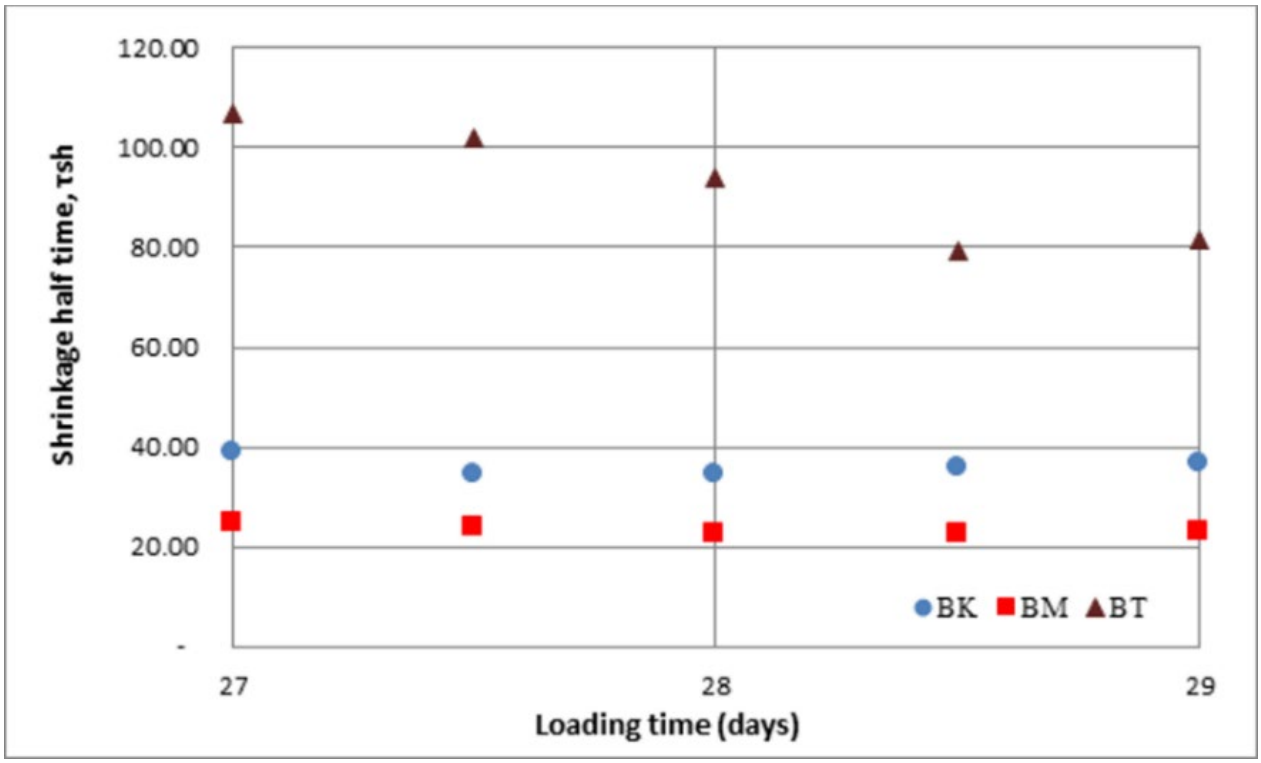

Figure 11. Shrinkage half-times (τ_{sh}) from tests.

Table 6. Average shrinkage half-times and K_{hs}.

Concrete Specimens	Average Shrinkage Half-Time (τ_{sh})	Coefficient K_{hs}
Kurik concrete (BK)	36,15	0.0089
Malind concrete (BM)	23,33	0,0056
Tanah Miring concrete (BT)	92,67	0,0195

Equation (5) and Table 6 were employed to replace Equation (4) to modify the B3 Model to predict concrete creep. The creep prediction of Merauke concrete and the creep test data for up to 364 days are presented in Figures 12–14. It can be seen that the modified B3 Model can estimate the actual creep data better than the original B3 Model. However, the difference between models and creep data in BT specimens is still obvious. Figure 11 shows that the variation in shrinkage half-time (τ_{sh}) values for BT specimens for days 27 to 29 are larger than those for other specimens. Better estimates of creep can be obtained when the half shrinkage constant (K_{hs}) is calculated with a small variation in shrinkage half-time (τ_{sh}) values, as shown for the specimens of BK and BM.

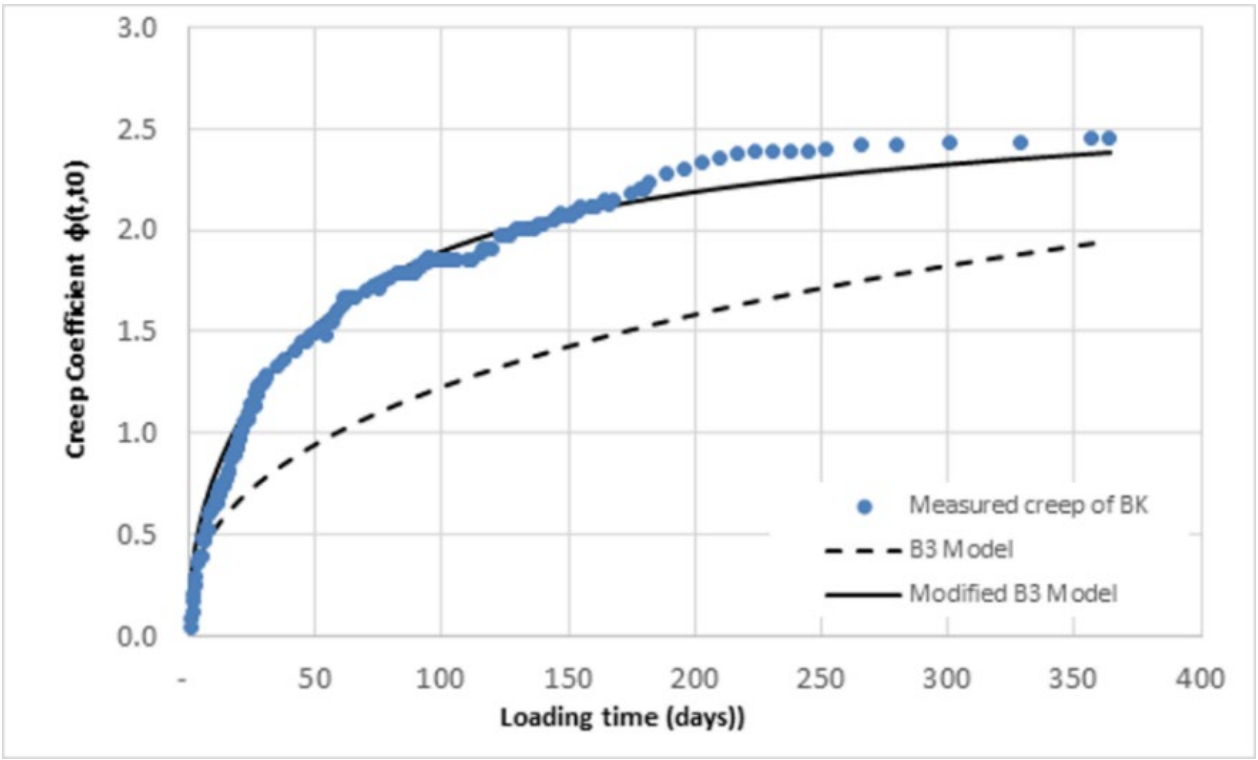

Figure 12. Comparison of creep models and measured creep of BK.

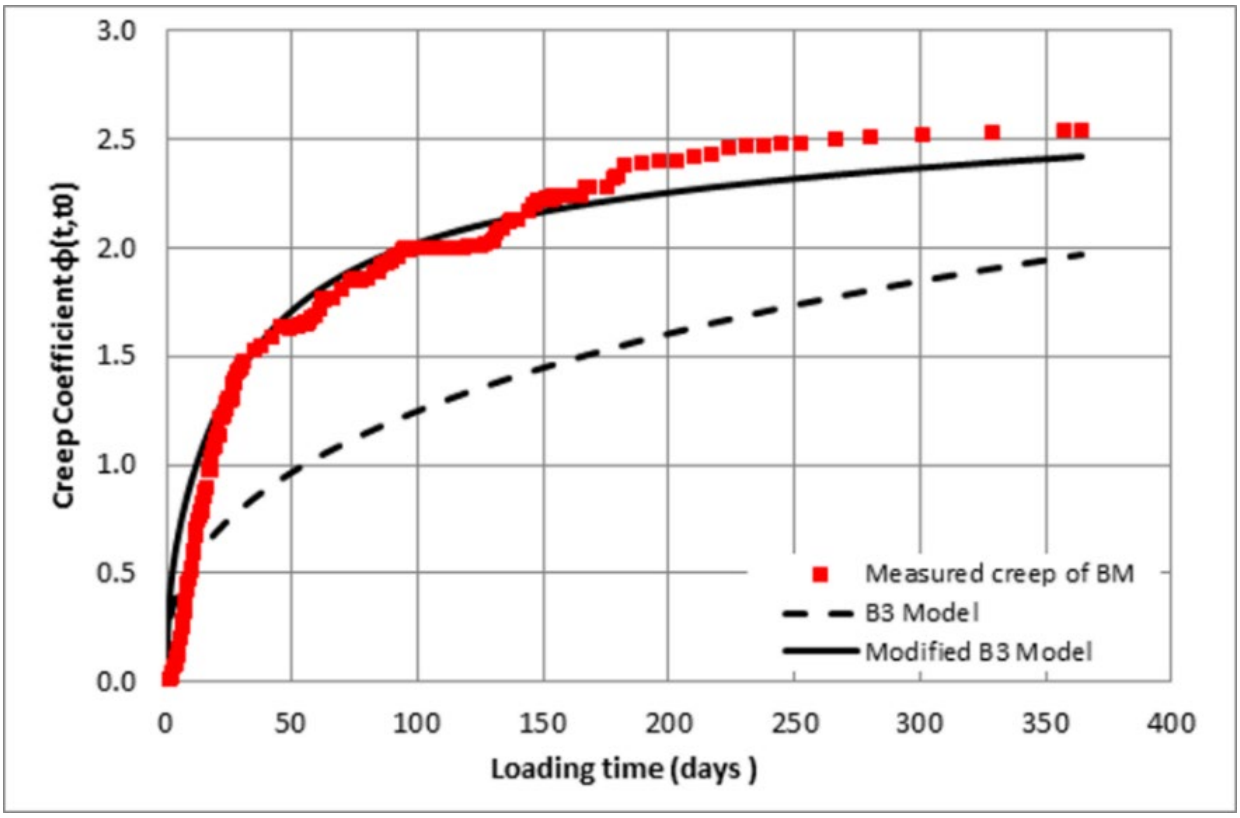

Figure 13. Comparison of creep models and measured creep of BM.

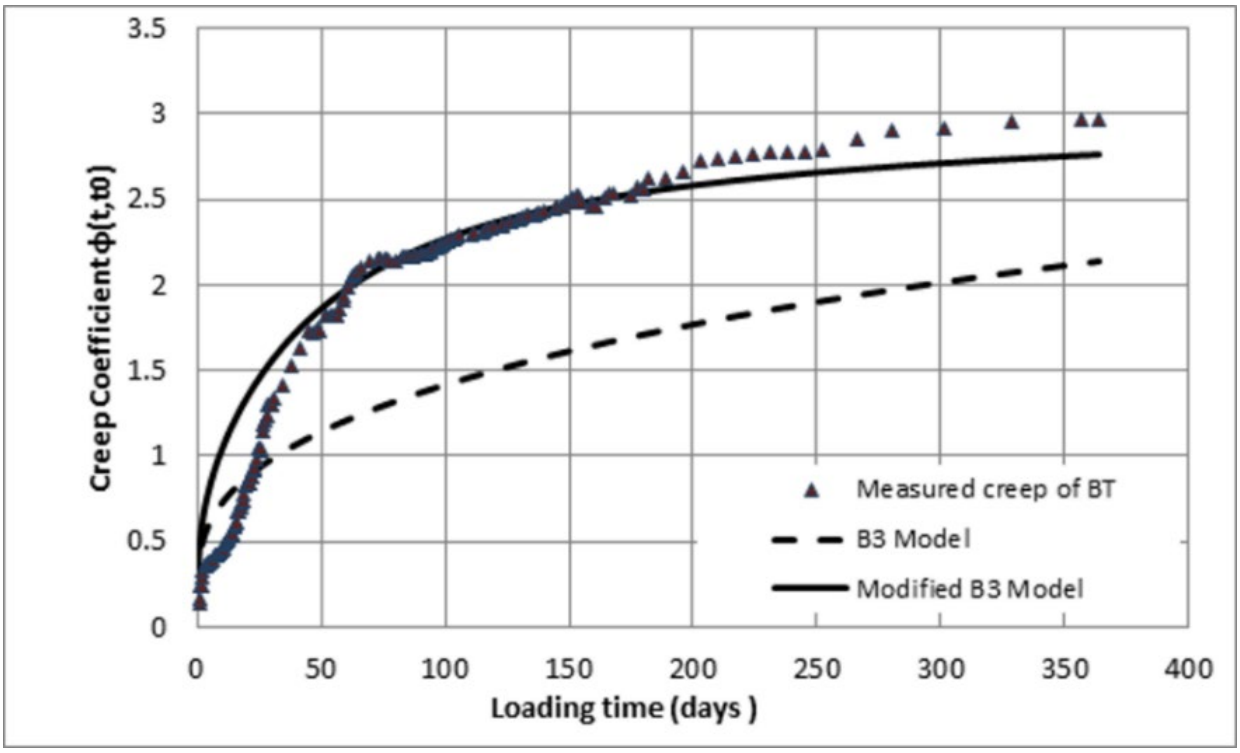

Figure 14. Comparison of creep models and measured creep of BT.

5. Conclusions

Shrinkage in concrete is influenced by the physical and chemical properties of the constituent materials. Concrete made from sand with high water absorption has a greater shrinkage value than concrete made from sand with low water absorption. Furthermore, sand with high CaO content is found to produce concrete with a lower shrinkage value.

Creep in concrete is influenced by the physical properties of sand: sand with a high percentage of fine grains exhibits more creep. In addition, the mud content also affects the creep in concrete. The results of compressive strength and modulus of elasticity of concrete showed that concrete with high compressive strength and a high modulus of elasticity tends to have less creep.

This research shows that concrete made from local sand in Kurik and Malind of Papua has potential to be used as structural concrete. However, further research is needed with different mix proportions to reduce creep deformation in the concrete from both sources.

A concrete creep prediction model has been developed based on the B3 Creep Model for estimating the creep of concrete made from pit sand. The modification was conducted by proposing a half-shrinkage constant K_{hs} as a material property. This constant can be obtained from short-duration creep tests. The creep parameters obtained from this test can be used to predict concrete creep better. The procedures presented in this paper can be reproduced for estimating creep on concrete made from local sand in other places.

Author Contributions: Conceptualization, D.A.P. and I.N.; methodology, D.A.P. and S.T.; validation, D.A.P.; investigation, D.A.P.; writing—original draft preparation, D.A.P.; writing—review and editing, I.N.; visualization, D.A.P.; supervision, S.T.; funding acquisition, D.A.P. and I.N. All authors have read and agreed to the published version of the manuscript.

Funding: This research was funded by Faculty of Engineering Diponegoro University, grant number 195/UN7.5.3.2/HK/2021.

Data Availability Statement: The details of the materials, methods and results have been provided in the paper. Hence, we are confident that the results can be reproduced. Readers interested in the calculation spreadsheet are encouraged to contact the authors by email.

Acknowledgments: The authors greatly acknowledge supports from the Materials and Structural Laboratory of Diponegoro University.

Conflicts of Interest: The authors declare no conflict of interest.

References

1. Brooks, J.J.; Megat Johari, M.A. Effect of Metakaolin on Creep and Shrinkage of Concrete. *Cem. Concr. Compos.* **2001**, *23*, 495–502. https://doi.org/10.1016/S0958-9465(00)00095-0.
2. Parsekian, G.A.; Barbosa, K.C.; Inforsato, T.B.; Deana, D.F.; Faria, M.S.; da Silva, C.O. Test Procedure for Shrinkage of Concrete Blocks. In Proceedings of the 10th Canadian Masonry Symposium, Banff, Alberta, 8–12 June 2005.
3. Huwae, D.D.M.; Parera, L.R.; Alpius; Tanijaya, J. The Use of Natural Sand from Lampusatu Beach, Kabupatenmerauke, Papua for Mixed Asphalt Concrete. *IOP Conf. Ser. Mater. Sci. Eng.* **2017**, *204*, 012022. https://doi.org/10.1088/1757-899X/204/1/012022.
4. Bédérina, M.; Khenfer, M.M.; Dheilly, R.M.; Quéneudec, M. Reuse of Local Sand: Effect of Limestone Filler Proportion on the Rheological and Mechanical Properties of Different Sand Concretes. *Cem. Concr. Res.* **2005**, *35*, 1172–1179. https://doi.org/10.1016/j.cemconres.2004.07.006.
5. Khouadjia, M.L.K.; Mezghiche, B.; Drissi, M. Experimental Evaluation of Workability and Compressive Strength of Concrete with Several Local Sand and Mineral Additions. *Constr. Build. Mater.* **2015**, *98*, 194–203. https://doi.org/10.1016/j.conbuildmat.2015.08.081.
6. Elat, E.; Pliya, P.; Pierre, A.; Mbessa, M.; Noumowé, A. Microstructure and Mechanical Behavior of Concrete Based on Crushed Sand Combined with Alluvial Sand. *CivilEng* **2020**, *1*, 181–197. https://doi.org/10.3390/civileng1030011.
7. Song, H.W., Song, Y.C., Byun, K.J., Kim, S.H. Modification of Creep-Prediction Equation of Concrete Utilizing Short-Term Creep Tests. In *SMIRT 16, Washington, DC, USA*; IASMiRT: Washington, DC, USA, 2001.
8. *ASTM C33-03*; Standard Spesification for Concrete Aggregate. ASTM International: Conshohocken, PA, USA, 2001; Volume 04.
9. Hasdemir, S.; Tuğrul, A.; Yilmaz, M. The Effect of Natural Sand Composition on Concrete Strength. *Constr. Build. Mater.* **2016**, *112*, 940–948. https://doi.org/10.1016/j.conbuildmat.2016.02.188.

10. Videla, C.; Carreira, D.J.; Garner, N. *ACI 209.2R-08: Guide for Modeling and Calculating Shrinkage and Creep*. ACI: Montreal, QC, Canada, 2008; ISBN 9780870312786;
11. *ASTM C512/C512M*; Standard Test Method for Creep of Concrete in Compression. ASTM International: Conshohocken, PA, USA, 2010; Volume 87, ISBN 9996758001.
12. Zhang, G.; Song, J.; Yang, J.; Liu, X. Performance of Mortar and Concrete Made with a Fine Aggregate of Desert Sand. *Build. Environ.* **2006**, *41*, 1478–1481. https://doi.org/10.1016/j.buildenv.2005.05.033.
13. Yilmaz, M.; Turul, A. The Effects of Different Sandstone Aggregates on Concrete Strength. *Constr. Build. Mater.* **2012**, *35*, 294–303. https://doi.org/10.1016/j.conbuildmat.2012.04.014.
14. Song, Y.; Wu, Q.; Agostini, F.; Skoczylas, F.; Bourbon, X. Concrete Shrinkage and Creep under Drying/Wetting Cycles. *Cem. Concr. Res.* **2021**, *140*, 106308. https://doi.org/10.1016/j.cemconres.2020.106308.
15. Revilla-Cuesta, V.; Evangelista, L.; de Brito, J.; Skaf, M.; Manso, J.M. Shrinkage Prediction of Recycled Aggregate Structural Concrete with Alternative Binders through Partial Correction Coefficients. *Cem. Concr. Compos.* **2022**, *129*, 104506. https://doi.org/10.1016/j.cemconcomp.2022.104506.
16. Boyd, A.J.; Skalny, J. Environmental Deterioration of Concrete. In *Environmental Deterioration of Materials*; WIT Press: Southampton, UK, 2007; Volume 28, pp. 143–184, ISBN 9781845640323.
17. Gedam, B.A.; Bhandari, N.M.; Upadhyay, A. Influence of Supplementary Cementitious Materials on Shrinkage, Creep, and Durability of High-Performance Concrete. *J. Mater. Civ. Eng.* **2016**, *28*, 04015173. https://doi.org/10.1061/(asce)mt.1943-5533.0001462.
18. Irfan-ul-Hassan, M.; Königsberger, M.; Reihsner, R.; Hellmich, C.; Pichler, B. How Water-Aggregate Interactions Affect Concrete Creep: Multiscale Analysis. *J. Nanomechanics Micromechanics* **2017**, *7*, 04017019. https://doi.org/10.1061/(asce)nm.2153-5477.0000135.
19. Akono, A.T.; Chen, J.; Zhan, M.; Shah, S.P. Basic Creep and Fracture Response of Fine Recycled Aggregate Concrete. *Constr. Build. Mater.* **2021**, *266*, 121107. https://doi.org/10.1016/j.conbuildmat.2020.121107.
20. Lasisi, F.; Osunade, J.A. Factors Affecting the Strength and Creep Properties of Laterized Concrete. *Build. Environ.* **1985**, *20*, 133–138. https://doi.org/10.1016/0360-1323(85)90008-3.
21. Bazant, Z.P.; Hauggaard, A.B.; Baweja, S.; Ulm, F.-J. Microprestress-Solidification Theory for Concrete Creep. I: Aging and Drying Effect. *J. og Eng. Mech.* **1997**, *123*, 1188–1194.
22. Granger, L.P.; Bažant, Z.P. Effect of Composition on Basic Creep of Concrete and Cement Paste. *J. Eng. Mech.* **1995**, *121*, 1261–1270. https://doi.org/10.1061/(asce)0733-9399(1995)121:11(1261).
23. Acker, P.; Ulm, F.J. Creep and Shrinkage of Concrete: Physical Origins and Practical Measurements. *Nucl. Eng. Des.* **2001**, *203*, 143–158. https://doi.org/10.1016/S0029-5493(00)00304-6.
24. Havlásek, P.; Šmilauer, V.; Dohnalová, L.; Sovják, R. Shrinkage-Induced Deformations and Creep of Structural Concrete: 1-Year Measurements and Numerical Prediction. *Cem. Concr. Res.* **2021**, *144*, 106402. https://doi.org/10.1016/j.cemconres.2021.106402.
25. Bazant, Z.P.; Baweja, S. Creep and Shrinkage Prediction Model for Analysis and Design of Concrete Structures-Model B3. *Mater. Struct. Constr.* **1995**, *28*, 357–365.
26. Bazant, Z.P. Mathematical Models for Creep and Shrinkage of Concrete. In *Creep and Shrinkage in Concrete Structures*; Wiley: Hoboken, NJ, USA, 1977; pp. 163–256.
27. Bažant, Z.P. Prediction of Concrete Creep and Shrinkage: Past, Present and Future. *Nucl. Eng. Des.* **2001**, *203*, 27–38. https://doi.org/10.1016/S0029-5493(00)00299-5.
28. Bazant, Z.P.; Baweja, S. Creep and Shrinkage Prediction Model for Analysis and Design of Concrete Structures: Model B3. *Am. Concr. Institute, ACI Spec. Publ.* **2000**, *194*, 1–83.
29. Harinadha Reddy, D.; Ramaswamy, A. Experimental and Numerical Modeling of Creep in Different Types of Concrete. *Heliyon* **2018**, *4*, e00698. https://doi.org/10.1016/j.heliyon.2018.e00698.
30. Nakov, D.; Markovski, G.; Arangjelovski, T.; Mark, P. Experimental and Analytical Analysis of Creep of Steel Fibre Reinforced Concrete. *Period. Polytech. Civ. Eng.* **2018**, *62*, 226–231. https://doi.org/10.3311/PPci.11184.
31. Torres, P.P.; Ghorbel, E.; Wardeh, G. Towards a New Analytical Creep Model for Cement-Based Concrete Using Design Standards Approach. *Buildings* **2021**, *11*, 155.